

Journal of Biomedical Optics

BiomedicalOptics.SPIEDigitalLibrary.org

Ultrahigh-speed optical coherence tomography utilizing all-optical 40 MHz swept-source

Tiancheng Huo
Chengming Wang
Xiao Zhang
Tianyuan Chen
Wenchao Liao
Wenxin Zhang
Shengnan Ai
Jui-Cheng Hsieh
Ping Xue

Ultrahigh-speed optical coherence tomography utilizing all-optical 40 MHz swept-source

Tiancheng Huo,[†] Chengming Wang,[†] Xiao Zhang, Tianyuan Chen, Wenchao Liao, Wenxin Zhang, Shengnan Ai, Jui-Cheng Hsieh, and Ping Xue*

Tsinghua University and Collaborative Innovation Center of Quantum Matter, Department of Physics, State Key Laboratory of Low-dimensional Quantum Physics and Center for Atomic and Molecular NanoSciences, Beijing 100084, China

Abstract. We present an ultrahigh-speed optical coherence tomography (OCT) based on an all-optical swept-source with an A-scan rate of 40 MHz. The inertia-free swept-source, which has its output power of 41.2 mW and tuning range of 40 nm and high scan linearity in wavenumber with Pearson's correlation coefficients r of 0.9996, consists of a supercontinuum laser, an optical band-pass filter, a linearly chirped fiber Bragg grating, an erbium-doped fiber amplifier, and two buffer stages. With sensitivity of 87 dB, high-speed OCT imaging of biological tissue *in vivo* is also demonstrated. © The Authors. Published by SPIE under a Creative Commons Attribution 3.0 Unported License. Distribution or reproduction of this work in whole or in part requires full attribution of the original publication, including its DOI. [DOI: 10.1117/1.JBO.20.3.030503]

Keywords: optical coherence tomography; swept-source; linearly chirped fiber Bragg grating.

Paper 140809LR received Dec. 5, 2014; accepted for publication Mar. 6, 2015; published online Mar. 24, 2015.

Optical coherence tomography (OCT) has attracted much attention since it was introduced in the 1990s.¹ Nowadays, there is an increasing need for volumetric imaging in real time, resulting in the demand for higher imaging speed.²⁻⁵ Swept-source OCT (SS-OCT) is an attractive and practical modality enabling an ultrahigh-speed A-scan rate. The Fourier domain mode locked laser and the microelectromechanical systems tunable vertical cavity surface-emitting laser have been developed as new light sources for SS-OCT enable high imaging speeds of up to 1 to 20 MHz.^{6,7} However, the mechanical moving parts of these swept-sources limit the response time and long-term stability. Recently, several high-speed inertia-free or all-optical swept-sources have been demonstrated. Okabe et al. presented an external-cavity swept-source equipped with a $\text{KTa}_{1-x}\text{Nb}_x\text{O}_3$ crystal deflector.⁸ Our group has also demonstrated a linear-in-wavenumber swept laser based on an acousto-optic deflector with a swept rate of ~ 2 MHz.⁹ Another approach to high speed all-optical swept-sources is based on a combination of

a broadband pulse source and a high-dispersion medium. Moon and Kim introduced an ultrahigh-speed SS-OCT with a stretched pulse supercontinuum source (SC) at a scanning rate of 5 MHz.¹⁰ Goda et al. reported a high-throughput OCT system with an A-scan rate of 90.9 MHz at 800 nm.¹¹ However, no OCT images of biological tissues were demonstrated in all these optical time-stretch swept-source-based OCT systems. Xu et al. demonstrated amplified optical time-stretch and all-fiber breathing laser-based all-optical ultrahigh-speed SS-OCT at an A-scan rate of 7.14 and 11.5 MHz, respectively.^{12,13} However, the effective A-scan rate of the former was only 1.2 MHz due to the averaging processes and the spectral shape of the latter swept-source was far away from the Gaussian shape as required for OCT imaging. Park et al.¹⁴ demonstrated an ultrahigh-speed optical frequency domain reflectometry system based on linearly chirped fiber Bragg gratings (LCFBGs) at 20 MHz repetition rate but with an output spectrum of only 9.2 nm, much less than needed for OCT. In this letter, we demonstrate all-optical SS-OCT based on the buffered optical time-stretch technique utilizing LCFBG as the dispersive medium and achieve a linear-in-wavenumber tuning range of 40 nm at an A-scan rate of 40 MHz.

The configuration of the swept-source is illustrated in Fig. 1. The SC with a pulse width of 150 ps, output power of 2 W, and spectrum of 460 to 2000 nm provides a broadband pulse train at a repetition rate of 10 MHz and is coupled into a single-mode fiber. Filtered by a circulator and LCFBG 1, the spectrum with a center wavelength of 1550 nm and full width at half maximum bandwidth of 52 nm enters the photonic time stretcher that consists of a circulator and LCFBG 2. The spectrum of each broadband pulse is converted into a temporal waveform by the large group velocity dispersion (GVD) of the LCFBG 2 with a duty cycle $< 25\%$. The buffer stages¹⁵ are used to fill up the duty cycle to 100% and further increase the swept rate with delayed copies of one scan by 4 \times . The erbium-doped fiber amplifier (EDFA) is integrated for shaping the spectrum and increasing the power to enhance the SS-OCT sensitivity. The basic parameters of the swept-source, including the bandwidth $\Delta\lambda$, time duration $\Delta\tau$, axial depth range Δz_{max} , and swept repetition rate R , are theoretically obtained.^{14,16,17} Though the bandwidth of the band-pass filter and the LCFBG 2 is 50 nm, the gain bandwidth of the EDFA is only 40 nm. Therefore, $\Delta\lambda$ is 40 nm and $\Delta\tau$ is revised as 19.8 ns. Thus, the theoretical axial resolution is 26 μm . The axial depth range Δz_{max} is generally limited by the GVD of the dispersive element, the sampling rate of the A/D converter, and the analog bandwidth (B) of the dual-balanced photo-detector, which are $-496 \text{ ps} \cdot \text{nm}^{-1}$, 2 GS/s, and 1.6 GHz, corresponding to the axial depth limits of 7.1, 0.59, and 0.47 mm, respectively. Considering all of the above limits, the theoretical axial depth range of our SS-OCT system is 0.47 mm. The buffering further increases the swept rate by 4 \times , therefore, the swept repetition rate R is 40 MHz. The time-stretch interferograms captured by the high-speed oscilloscope are shown in Fig. 2(a). Without any calibrations,¹² the temporal swept waveform (short dot line) dramatically shows a good agreement with the spectrum (solid line) captured by an optical spectrum analyzer, as shown in Fig. 2(b). With a total GVD of $-496 \text{ ps} \cdot \text{nm}^{-1}$, the full-swept range of 40 nm is mapped into a time span of 21 ns, which is consistent with the theoretical value of 19.8 ns, corresponding to a $\sim 100\%$ duty cycle. The optical power from the LCFBG 1 is ~ 1 mW, which extremely limits the system sensitivity. Therefore, optical amplification, i.e., EDFA, is necessary.

*Address all correspondence to: Ping Xue, E-mail: xuep@tsinghua.edu.cn

[†]The first two authors contributed equally to this paper.

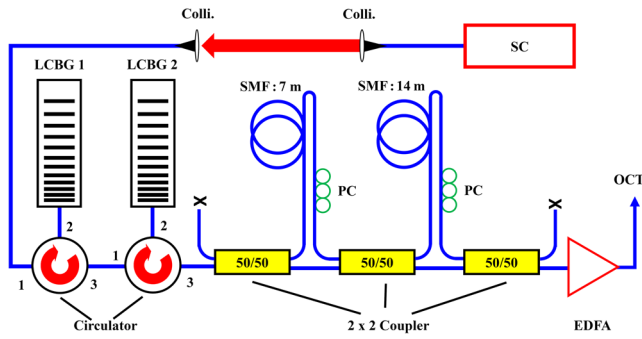


Fig. 1 Schematic of the buffered optical time-stretch-based 40 MHz swept-source. SC, supercontinuum source; colli, collimator; SMF, single-mode fiber; PC, polarization controller.

With $\sim 38 \mu\text{W}$ power input in EDFA, the output of the 40 MHz swept-source is 41.2 mW.

We use a flat mirror at the sample position of $50 \mu\text{m}$ to evaluate the point spread function (PSF). The optical power incident on the specimen is $\sim 25.5 \text{ mW}$ for 40 MHz SS-OCT with a theoretical sensitivity of 90 dB. The measured axial resolution by the PSF is $27 \mu\text{m}$, in good agreement with the theoretical calculation of $26 \mu\text{m}$. The sensitivity is measured with a 1% negative differential conductivity filter in the sample arm. As shown in Fig. 3(a), the sensitivity of the 40 MHz system is 86.7 dB, only 3.3 dB below the theoretical limit, implying that the overall performance of the system including the swept source is good. The sensitivity limitations are due to the limited optical power, the inevitable insertion losses of all the fiber components, the spectral fluctuation of the broadband source, and the noise of the EDFA. Limited sampling rate of the A/D converter may also reduce the quality of the OCT image due to the sparse data points at a high A-scan rate of 40 MHz. To further improve the image quality for clinical applications, higher optical power, more stable pumping for the SC source, and a faster A/D converter are to be employed in future. We plot the different PSFs by varying the mirror position, as shown in Fig. 3(b). The -6 dB imaging depth is 0.42 mm , also in good agreement with the theoretical depth range of 0.47 mm .

Based on the principles of the optical time-stretch technique,^{14,16,17} the one-to-one mapping between the optical frequency (ω) and the time (T) in the reference frame of the pulse that propagates at the group velocity is given by $T(\omega) = \beta_2(\omega - \omega_0)z$, where ω_0 is the central optical frequency, z is the propagation distance, and β_2 is the second-order dispersion coefficient. Because LCFBGs provide a practically

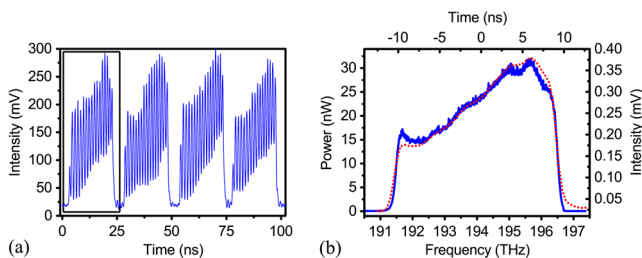


Fig. 2 (a) 40 MHz real-time time-stretch interferograms. The signal in the solid rectangle is the original fringes, and the later three are its copy by the buffer stages. (b) Raw spectra after the LCFBG2 are captured by an optical spectrum analyzer (solid line) and by a high-speed oscilloscope (short dotted line).

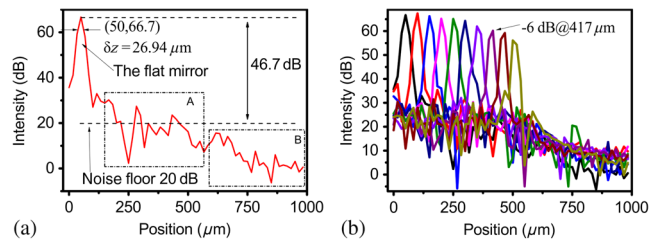


Fig. 3 (a) Measured point spread function (PSF) on a logarithmic scale at a position of $50 \mu\text{m}$ with a -6 dB axial resolution of $26.9 \mu\text{m}$ and sensitivity of 86.7 dB. The noise floor is calculated from the points in the A rectangle, as the points in the B rectangle are out of the bandwidth limits of the photo-detector. (b) Fall-off performance of the swept-source optical coherence tomography (SS-OCT).

flat gain and linear group delay, β_2 is almost a constant. Therefore, the swept-source scans the wavenumber linearly with time. In Fig. 4(a), the wavenumber versus time curve (dashed line) is obtained from the fringes (solid line) at a 40 MHz swept rate with a fiber-based Mach-Zehnder interferometer, in which the arm difference is set to be $\sim 0.1 \text{ mm}$. The Pearson's r is 0.9996 in the fitted linear curve (short dotted line). The integrated relative frequency error χ , defined as a measure for the swept linearity,¹⁸ is 0.0002, as shown in Fig. 4(b).

To illustrate the performance of the 40 MHz swept-source, SS-OCT imaging of the intralipid injected into a glass tube and human palm is implemented, as shown in Figs. 5(c) and 5(d). Due to the analog bandwidth upper limit of the acquisition system, the recordable imaging depth is not enough for viewing the whole cross section of the tube. Therefore, in comparison, a 10 MHz swept-source-based SS-OCT imaging with a fourfold larger imaging depth is also given, as shown in Figs. 5(a) and 5(b). The configuration of the 10 and 40 MHz swept-source is almost the same, except that the LCFBG2 in the 40 MHz swept-source is replaced by LCFBG 3 and the buffered stage is removed in the 10 MHz swept-source. With an input power of $\sim 38 \mu\text{W}$ in the EDFA, the output power of the 10 MHz swept-source is 40.5 mW. The optical power incident on the specimen is $\sim 25.1 \text{ mW}$ for 10 MHz SS-OCT with the theoretical sensitivity of 90 dB. With a total GVD of $-2312 \text{ ps} \cdot \text{nm}^{-1}$, its full-swept range of 40 nm is mapped into a time span of 91.2 ns. The axial resolution, -6 dB imaging depth, and sensitivity of the 10 MHz SS-OCT are $27 \mu\text{m}$, 1.95 mm, and 85.5 dB, respectively.

It is worthwhile to mention that all imaging is implemented without any averaging¹² of the consecutive A-scan signal. As shown in Fig. 5, our ultrahigh-speed SS-OCT can clearly reveal the structure of the epidermis and dermis layers. With a faster photo-detector and data acquisition card, the maximum imaging

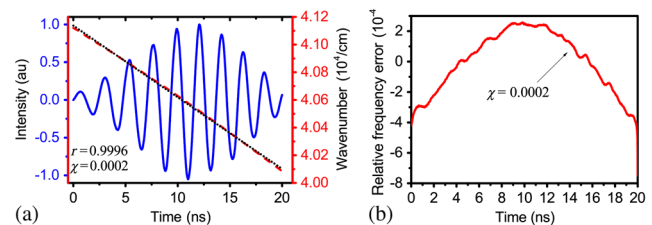


Fig. 4 (a) Fringes (with Gaussian window, solid line), the wavenumber versus time curve (dashed line) and its linear fit (short dotted line); (b) relative frequency error curve of the 40 MHz swept-source.

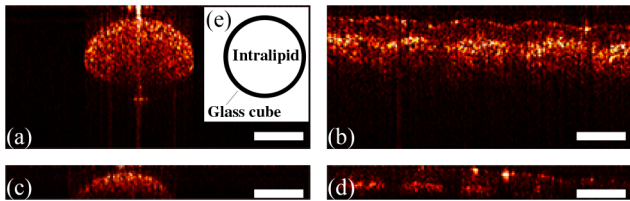


Fig. 5 Two-dimensional (2-D) cross-sectional imaging of intralipid injected into a glass cube by (a) (423×200 pixels) 10 MHz swept-source and (c) (423×50 pixels) 40 MHz swept-source. 2-D cross-sectional imaging of human palm by (b) (564×200 pixels) 10 MHz swept-source and (d) (564×50 pixels) 40 MHz swept-source. The scale bar represents $500 \mu\text{m}$. (e) Schematic for the sample in (a) and (c). The intralipid was injected into a glass tube with an outer diameter of 1.2 mm and inner diameter of ~ 1 mm.

depth could reach ~ 7 mm, as implied by the quality of the image in Fig. 5, because the signal in the deep depth does not have much falloff. Meanwhile, it is possible to superimpose more LCFBGs to enlarge the spectral range and to achieve higher axial resolution.

In summary, a 40 MHz all-optical swept-source at 1545 nm with a 3 dB tuning range of 40 nm, output power of 41.2 mW, and EDFA amplification is developed and achieves good wave-number-linearity with Pearson's r of 0.9996 and integrated relative frequency error of 0.0002. With a sensitivity of 87 dB, 6 dB fall-off depth of 0.42 mm, and A-scan rate of 40 MHz, ultrahigh-speed SS-OCT imaging of biological tissue *in vivo* is demonstrated.

Acknowledgments

This work is supported in part by the National Natural Science Foundation of China under Grant No. 61227807 and by the Tsinghua Initiative Scientific Research Program under Grant No. 2013THZ02-3.

References

1. D. Huang et al., "Optical coherence tomography," *Science* **254**, 1178–1181 (1991).

2. M. Wojtkowski et al., "In vivo human retinal imaging by Fourier domain optical coherence tomography," *J. Biomed. Opt.* **7**(3), 457–463 (2002).
3. M. A. Choma, K. Hsu, and J. A. Izatt, "Swept source optical coherence tomography using an all-fiber 1300 nm ring laser source," *J. Biomed. Opt.* **10**, 044009 (2005).
4. R. Wang et al., "Megahertz streak-mode Fourier domain optical coherence tomography," *J. Biomed. Opt.* **16**, 066016 (2011).
5. D. Choi et al., "Fourier-domain optical coherence tomography using optical demultiplexers imaging at 60,000,000 lines/s," *Opt. Lett.* **33**, 1318–1320 (2008).
6. W. Wieser et al., "Multi-megahertz OCT: high quality 3D imaging at 20 million A-scans and 4.5 GVoxels per second," *Opt. Express* **18**, 14685–14704 (2010).
7. O. O. Ahsen et al., "Swept source optical coherence microscopy using a 1310 nm VCSEL light source," *Opt. Express* **21**, 18021–18033 (2013).
8. Y. Okabe et al., "200 kHz swept light source equipped with KTN deflector for optical coherence tomography," *Electron. Lett.* **48**, 201–202 (2012).
9. T. Huo et al., "Linear-in-wavenumber swept laser with an acousto-optic deflector for optical coherence tomography," *Opt. Lett.* **39**, 247–250 (2014).
10. S. Moon and D. Y. Kim, "Ultra-high-speed optical coherence tomography with a stretched pulse supercontinuum source," *Opt. Express* **14**, 11575–11584 (2006).
11. K. Goda et al., "High-throughput optical coherence tomography at 800 nm," *Opt. Express* **20**, 19612–19617 (2012).
12. J. Xu et al., "Megahertz all-optical swept-source optical coherence tomography based on broadband amplified optical time-stretch," *Opt. Lett.* **39**, 622–625 (2014).
13. X. Wei et al., "Breathing laser as an inertia-free swept source for high-quality ultrafast optical bioimaging," *Opt. Lett.* **39**, 6593–6596 (2014).
14. Y. Park et al., "Optical frequency domain reflectometry based on real-time Fourier transformation," *Opt. Express* **15**, 4597–4616 (2007).
15. R. Huber, D. C. Adler, and J. G. Fujimoto, "Buffered Fourier domain mode locking: unidirectional swept laser sources for optical coherence tomography imaging at 370,000 lines/s," *Opt. Lett.* **31**, 2975–2977 (2006).
16. K. Goda and B. Jalali, "Dispersive Fourier transformation for fast continuous single-shot measurements," *Nat. Photonics* **7**, 102–112 (2013).
17. G. Hausler and M. W. Lindner, "Coherence radar and spectral radar-new tools for dermatological diagnosis," *J. Biomed. Opt.* **3**(1), 21–31 (1998).
18. C. M. Eigenwillig et al., "K-space linear Fourier domain mode locked laser and applications for optical coherence tomography," *Opt. Express* **16**, 8916–8937 (2008).